A model for catchment soil erosion management in humid agricultural environments.

Andrés Peñuela[1*], Haykel Sellami[2], Hugh G. Smith[1]

[1]School of Environmental Sciences, University of Liverpool, Roxby Building L69 7ZT

[2]Laboratory of Georesources, Centre for Water Research and Technologies, BorjCedria, Tunisia

*Corresponding author: A.Penuela-Fernandez@liverpool.ac.uk

ABSTRACT: Intensive agricultural practices have critically contributed to the global increase in soil erosion and sediment fluxes. To reduce the impact of these practices, models able to represent the effect of changes in agricultural land use, farming and conservation practices are needed. Moreover, simulations spanning multi-decadal periods can overcome the potentially confounding influence of climate variability on shorter-term studies of impacts from agricultural change. Conceptual erosion models, such as the Morgan-Morgan-Finney model (MMF), allow simulation of soil erosion rates and sediment fluxes over longer periods, while still retaining a general description of runoff and sediment generation processes. In addition, the Modified MMF (MMMF) offers improved representation of vegetation cover effects through measurable plant properties. However, as an annual model, MMF does not capture seasonal variability in climate, hydrology and land cover. Here, we propose a new model for humid environments based on the MMF to address its limitations and improve its predictive ability, while retaining its simplicity and low computational and parameterisation requirements. This includes monthly computation, representation of catchment hydrology based on delineation of saturated areas according to the topographic wetness index (TWI), and improved representation of ground and vegetation cover effects. The proposed model, MMF-TWI, was applied in an agricultural catchment in the UK and performance compared to published data and MMMF simulation results. Land cover spatial and temporal variability, crop type as well as farming and conservation practices were found to have a significant influence on simulated sediment yields. Our findings demonstrate: a) that MMF-TWI improves predictive ability compared to MMMF in humid environments, b) the importance

of capturing sub-annual variability in climate, saturated areas and land cover, c) the ability of MMF-TWI to represent impacts from farming and conservation practices, and d) the potential for MMF-TWI to be applied as a soil erosion management tool.

Introduction

Soil erosion is widely recognized as the main cause of soil degradation in agricultural areas (Pimentel et al., 1995, Lal, 2001, Morgan, 2005, Pimentel, 2006). This not only produces important economic costs but also contributes to the contamination of streams and water bodies (Stoate et al., 2001, Pimentel, 2006). In agricultural catchments, intensive crop cultivation and overgrazing have important impacts on soil erosion. Cultivation results in periods of soil surface exposure to direct raindrop impact (Morgan, 2005, Durán Zuazo and Rodríguez Pleguezuelo, 2008) and intensive tillage in arable lands and overgrazing may degrade soil structure and reduce ground cover (Evans, 1997, Pietola et al., 2005). Thus, in agricultural fields, the hydrological response and hence, the magnitude of erosion can change significantly throughout the year due to seasonal changes in climate, soil moisture and ground cover (Fiener et al., 2011). Inter-year variability in crop cover as well as longer-term land cover changes linked to multi-decadal trends in agricultural production also affect catchment sediment yields (Foster et al., 2011, Smith et al., 2014). Besides temporal variation, the spatial arrangement of land cover is another factor that can have important effects on catchment sediment yield (Van Oost et al., 2000, Sharma et al., 2011, Zhang et al., 2017). Spatial variation in cover is more likely to occur over longer periods and also when strategically placed conservation measures, such as buffer strips along the stream network, are applied. Temporal variability in land use and management interacts with the spatial distribution across the catchment to influence the extent of connectivity between sediment generating areas and surface water bodies (Bracken and Croke, 2007, Lexartza-Artza and Wainwright, 2009). Hence, land cover and its inter- and intra-year variability and spatial arrangement are important factors whose

effects must be captured by models for catchment management and soil conservation purposes.

Overland flow provides a hydrological connection between the landscape and surface water bodies. Since overland flow carries sediment eroded on hillslopes, runoff-prone areas are potentially the most important sediment contributing areas in a catchment. In humid regions such as the UK and in landscapes with shallow restrictive soils, saturation excess is considered as the characteristic mechanism of runoff generation (Dunne and Black, 1970, Dunne et al., 1975, Walter et al., 2000). According to this mechanism local saturation occurs in areas where the upslope drainage flux exceeds the capacity of the soil profile to transmit the flux (O'Loughlin, 1981) and rain that falls on saturated areas becomes overland flow. Because the saturated areas vary in extent during rainfall events and seasonally, saturation excess runoff is associated with the variable source area concept (VSA; Hewlett and Hibbert, 1967; Frankenberger et al., 1999). During wet periods the upslope drainage is higher and enlarges the area prone to saturation and hence to overland flow generation; whilst during dry periods the extent of these areas decreases. In water quality hydrology, these overland flow prone areas are called hydrological sensitive areas (HSAs) and they are considered the main source of sediments and pollutants to surface water bodies (Walter et al., 2000). Therefore, it is crucial to estimate the HSAs in order to identify the sediment contributing areas and hence, to properly simulate the overland flow and sediment flux processes in a catchment. A number of studies have shown that the distribution of wetness (Beven and Kirkby, 1979, O'Loughlin, 1981, Moore et al., 1988, Beven et al., 1995) and overland flow prone areas (O'Loughlin, 1986, Dietrich et al., 1992, Agnew et al., 2006, Thomas et al., 2016) can be predicted by means of the topographic wetness index (TWI; Beven and Kirkby, 1979; Beven, 1986).

To achieve good prediction of soil erosion and sediment fluxes and an adequate representation of hydrological/erosion processes, models must be able to capture not only the spatial but also the temporal distribution and variability of the most relevant factors, such as the farming and conservation practices, vegetation cover and climate. Re-vegetation is a widely accepted method for controlling soil erosion by intercepting rainfall and runoff (Durán Zuazo and Rodríguez Pleguezuelo, 2008). However, farming practices, such

as crop rotation, cover crops and soil tillage, and crop growth produce important seasonal variations in the level of soil erosion protection provided by plant cover. The level of canopy cover protection, which reduces the direct impact of rain drops on the soil surface, changes according to the type of crop and the plant growth stage. For instance, the duration and initiation date of the 'window of opportunity' for erosion, i.e. the period when the soil is bare or the crop is still not well established, greatly influence the risk of erosion (Kirkbride and Reeves, 1993, Boardman and Favis-Mortlock, 2014). Tillage practices in arable fields can have important impacts on soil structure and surface residues and hence on soil erosion. On the one hand, conventional tillage buries or removes crop residues and loosens the soil so that it is easily detached and removed by the overland flow. On the other hand, conservation tillage, no-tillage and cover cropping can reduce soil erosion by allowing more surface residue and limiting soil structure degradation (Carter, 1994, Holland, 2004, Busari et al., 2015).

A number of process-based erosion models, such as WEPP (Nearing et al., 1989) and EUROSEM (Morgan et al., 1998) are able to simulate the effects of vegetation cover and farming practices. This type of model is data and computer time demanding which makes them suitable for simulation of single events and for small areas but not for longer-term simulations and large areas (Merritt et al., 2003). Conversely, less computational and data demanding empirically based models are better suited for larger areas and long-term simulations, and hence for management and soil conservation purposes. Empirical models are useful for identifying sources of sediment and predicting sediment delivery at the catchment scale and have even shown higher model efficiencies than process based models (Tiwari et al., 2000). However, they are based on empirical relationships that rely on results observed in certain regions and conditions that may not be extrapolated confidently to other areas (Prosser et al., 2001). In order to improve our understanding of downstream impacts of land use change and hence to improve catchment management and soil conservation practices, models able to represent and predict in a simple manner patterns of sediment delivery are needed. Conceptual models provide a compromise between empirical and process based soil erosion models. While keeping relatively low computational and data requirements, these models incorporate a general description of the main catchment processes (Merritt et

al., 2003). This makes conceptual models potentially better able to represent and predict sediment delivery rates and to identify contributing areas over long time periods and at the catchment scale.

An example of a conceptual soil erosion model is the Morgan-Morgan-Finney model (MMF; Morgan et al. (1984)) including its Revised (RMMF; Morgan (2001)) and Modified (MMMF; Morgan and Duzant (2008)) versions. It has been applied in a variety of climate regions, land use types and scales (De Jong et al., 1999, Vigiak et al., 2005, López-Vicente et al., 2008, Vieira et al., 2014, Li et al., 2017). This model retains the simplicity of empirical models yet has a stronger physical base. MMF separates erosion into the water and sediment phases and applies different equations to describe the mechanisms of runoff generation, soil detachment and sediment transport with a relatively low number of parameters. Since guide values for the parameters are provided and it requires readily available data, MMF can be potentially used without the need for calibration. In the most recent version of MMF, modifications were made to represent the effects of vegetation cover through measurable plant parameters and to improve representation of the processes of soil detachment (Morgan, 2001), sediment transport and sedimentation, as well as sediment routing (Morgan and Duzant, 2008). These characteristics make MMF potentially suitable for longer-term studies of the impacts of catchment land use change on soil erosion and sediment delivery. However, as an annual model, it does not take into account intra-year variations in climate and crop cover, and hence it is not able to represent, for instance, low crop cover periods and the effect of heavy rainfall during these periods. The model also assumes that the whole catchment is contributing to sediment delivery, but in humid regions only saturated areas are likely to generate runoff and hence become sediment contributing areas. Moreover, poor performance of the MMF model in predicting runoff has been reported (Vigiak et al., 2005, Morgan and Duzant, 2008) and needs to be improved.

The objective of this paper is to propose a conceptual soil erosion model for humid environments based on the MMF model that overcomes the above mentioned limitations by improving representation of (1) spatial and temporal variability in land cover resulting from both natural processes and farming practices and (2) seasonal variations in climate, runoff generation, and

sediment contributing areas. Another important objective of this study is to introduce these developments and, yet, retain the simplicity of MMF and its low computational and parameterization requirements. This is intended to support new applications of the model for land management purposes as well as longer-term simulations of catchment soil erosion spanning decades to centuries.

Model description

The Morgan-Morgan-Finney model

The MMF model (Morgan et al., 1984) separates the erosion process into two phases: water and sediment. In the water phase, overland flow is estimated as an exponential function of the rainfall volume and takes into account plant interception, topography and soil water storage. The energy available for soil detachment is derived from rainfall and plant interception and the transport capacity from the volume of overland flow, slope gradient and cover management. The model uses the Meyer and Wischmeier (1969) scheme in which the sediment production, i.e. detached, is compared to the transport capacity and the lower value is taken as the sediment transport rate. The Revised version (RMMF) incorporated the process of flow detachment and the effect of plant height on the energy available for soil detachment (Morgan, 2001). The subsequent Modified version (MMMF) incorporated soil particle-size selectivity, sediment deposition and vegetation cover effects (Morgan and Duzant, 2008).

MMF-TWI

In the present study, we modify the representation of the soil-water balance and runoff generation in MMF to produce the new model, MMF-TWI. This integrates a soil moisture sub-model and a crop-growth sub-model. The soil moisture sub-model is a simple approach based on daily soil saturation-excess which uses the TWI to represent interflow movement and to delineate

monthly topographic saturated areas, similar to the method used by O'Loughlin (1986) or the DREAM model (Manfreda et al., 2005). Monthly overland flow is then only generated where rain falls on saturated areas, which are considered as sediment contributing areas (Figure 1). MMF-TWI should be applied in humid regions where saturation excess is the characteristic mechanism of overland flow generation. Crop growth simulation is used to generate daily canopy cover and plant interception parameters (Neitsch et al., 2011). This captures intra-year variations in canopy cover related to crop type, planting time, plant growth rates, harvesting and crop rotations.

MMF-TWI takes into account intra-year plant growth and seasonal variability of parameters affected by changes in vegetation cover and predicts the intra-year variability of soil loss and sediment deposition by applying a monthly time step. While the soil moisture and plant growth sub-models need daily rainfall and temperature data, respectively, and a daily computation time step, both the hydrological and soil erosion components of MMF-TWI use a monthly time step (Figure 1) to capture seasonality while keeping the computational requirements low. It must be noted that, while soil erosion and sediment fluxes are computed on a monthly basis, the outputs of MMF-TWI are reported on an annual basis.

Several equations and parameters are modified from the previous versions of MMF to improve the representation of physical processes and the effects of agricultural practices. These include changes to the net rainfall (Rf) equation (Eq. 1 in Morgan and Duzant (2008)) to correct the slope adjustment factor (Choi et al., 2016) and computation of canopy cover (CC), plant height (PH) and plant interception (PI) on a monthly basis by the new crop growth and soil moisture sub-models. Ground cover is now computed by applying the surface ground cover subfactor (SC) used in RUSLE and a tillage factor (TF) to represent tillage practices and these factors are incorporated into the equations representing detachment of soil particles by raindrop impact and runoff (Eq. 14, 15 , 16 and Eq. 18, 19, 20 in Morgan and Duzant (2008)). We also replace the flow velocity ratio in the transport capacity equations (Eq. 39, 40 , 41 in Morgan and Duzant (2008)) with SC and TF. We correct the error in the kinetic energy (KE) of leaf drainage (LD) equation in RMMF (Morgan, 2001) that has propagated to MMMF (Eq. 6 in Morgan and Duzant (2008)) and several other

models based on MMF, including PSYCHIC (Davison et al., 2008) and SERT (López-Vicente et al., 2013). This correction incorporates the amount of leaf drainage (LD) into the KE(LD) equation, originally proposed by Brandt (1990). The maximum value of the plant height (PH) in the KE(LD) equation is limited by the raindrop terminal velocity height (Satterlund and Adams (1992). We also incorporate an understorey effect in reducing KE for woodland cover types (evergreen and deciduous).

Plant growth sub-model

Plant growth is modelled to determine daily canopy cover and plant height. We adopt the SWAT model (Neitsch et al., 2011) approach where Leaf Area Index (LAI) is estimated as a function of the Heat Unit concept (Boswell, 1926) and crop planting and harvesting dates (Neitsch et al., 2011). Initial parameter values were drawn from the SWAT database (Arnold et al., 2012). Plant growth/decay rate depends on the daily temperature and the dormancy period of the plant. A Heat Unit (HU) accumulates when the mean daily temperature (T_{day}) exceeds the minimum temperature (T_{base}) for plant growth (Eq. 1). HU's are summed until reaching the total HU's required for maturity (PHU).

$$HU = T_{day} - T_{base}, \qquad where\ T_{day} > T_{base} \tag{1}$$

Plants enter a period of winter dormancy when the daylength is shorter than the minimum daylength for growth, which depends on the latitude of the catchment, and a period of summer dormancy, when the soil moisture drops below the wilting point.

The daily increase in LAI with plant growth is related to the accumulated *HU*'s required to reach maturity according to Eq. 2:

$$F_{LAI} = \frac{F_{PHU}}{F_{PHU} + e^{(L_1 + L_2 . F_{PHU})}}, \qquad where\ F_{PHU} = \frac{\sum_{i=1}^{d} HU_i}{PHU} \tag{2}$$

in which F_{LAI} is the fraction of the plant's maximum LAI (LAI_{max}) corresponding to the fraction of accumulated HU's (F_{PHU}) on a given day relative to the total potential heat units required for maturity (PHU). L_1 and L_2 are shape coefficients calculated using plant growth parameter values for two known points related to F_{LAI} and F_{PHU} (Neitsch et al., 2011). The change in *LAI* per day is calculated from Eq. 3:

$$\Delta LAI_i = LAI_{max}\left(F_{LAI,i} - F_{LAI,i-1}\right)\left(1 - e^{(5(LAI_{i-1} - LAI_{max}))}\right) \quad (3)$$

Once the maximum LAI is reached, the LAI remains constant until LAI declines during the period dominated by leaf senescence ($F_{PHU,sen}$) according to Eq. 4:

$$LAI_i = 16\, LAI_{max}\,(1 - F_{PHU})^2, \qquad where\ F_{PHU} > F_{PHU,sen} \quad (4)$$

The canopy cover (CC; Figure 2) is derived from the LAI using Beer's law and assuming that the proportion of light intercepted by plants (L_{int}) is equal to the fractional land surface covered by canopy (Eq. 5; Eagleson, 1982):

$$CC = L_{int} = 1 - e^{-k\,LAI} \quad (5)$$

where *k* is the light extinction coefficient. The canopy height (h_c, m) on a given day is calculated from Eq. 6:

$$h_c = h_{c,max}\sqrt{F_{LAI}} \quad (6)$$

where $h_{c,max}$ is the maximum canopy height for the plant.

For permanent covers, such as grassland and evergreen woodland, the MORECS model approach (Hough and Jones, 1997) is adopted. For grassland, LAI and hence CC, is modelled as a stepwise evolution (Figure 2c) and for evergreen woodland as a constant value throughout the year.

Soil moisture sub-model

A simple soil moisture sub-model based on soil saturation-excess was used to calculate daily actual evaporation, soil moisture, soil water deficit and runoff. The sub-model computes the net precipitation, i.e. the volume of rainfall that is not lost by interception and evaporation from leaves of the plants. Net precipitation reaches the soil surface directly from precipitation (throughfall), by dripping from the canopy or channelled along the stem or trunk. Daily permanent plant interception (*PI*; mm) was determined as a function of *LAI* and *CC*, both computed from the plant growth sub-model. For this purpose, Eq. 7, an empirical equation proposed by Braden (1985) that relates *LAI*, *CC* and gross daily rainfall (*R*; mm), was applied:

$$PI = a\,LAI\,(1 - \frac{1}{1 + \frac{CC\,R}{a\,LAI}}) \quad (7)$$

where a is an empirical coefficient that ranges between 0.3, before senescence and 0.6 at the end of the senescence period (Braden, 1995). In this study, we assume a constant value equal to 0.4 in order to account for the senescence period, during which leaves can store more water on their surface. In woodland areas, the canopy cover and hence the plant interception is represented by two layers: the tree canopy and the understorey canopy. Eq. 7 is first applied to compute the tree interception and the net rainfall below the tree canopy, which is then used to compute the understorey interception and hence, the net rainfall that reaches the soil surface.

Net rainfall is computed as:

$$Rf = R\,(1 - PI)\cos\,\beta \quad (8)$$

where β is the slope angle in degrees. This equation includes the correction to the slope angle effect proposed by Choi et al. (2016).

The soil moisture sub-model computes the daily volume of water stored in the soil (S_t; mm) by taking into account the antecedent volume of water

stored in the soil (S_{t-1}), net precipitation (*Rf*; mm), evapotranspiration (*ET*; mm), saturation excess runoff (*Q*; mm) and deep percolation (*Dp*; mm). The function applied to compute the daily volume of water stored in the soil in its general form is:

$$S_t = S_{t-1} + Rf - ET - Q - Dp \quad (9)$$

Similar to the DREAM model (Manfreda et al., 2005) and SWAP model (Kroes et al., 2008) approaches, *ET* is calculated as a combination of the actual evapotranspiration from the vegetated fraction (*CC*) and the actual evaporation from the bare soil fraction (1 - *CC*):

$$ET = ET_{veg}\, CC + E_{soil}(1 - CC) \quad (10)$$

where ET_{veg} is the actual daily evapotranspiration from the vegetated fraction (mm) and E_{soil} the actual daily evaporation of the bare soil fraction (mm). Both ET_{veg} and E_{soil} depend on the degree of water availability in the soil. The degree of water availability is expressed by actual soil moisture divided by field capacity soil moisture. This approach is based on the following assumptions (Bergström and Singh, 1995):

- if S_{t-1} is higher than the volume of water stored in the soil at field capacity:

$$ET_{veg} = PE_{veg} \quad (11)$$

$$E_{soil} = PE \quad (12)$$

- if S_{t-1} is lower than the volume of water stored in the soil at field capacity (S_{fc}) and higher than at the wilting point (S_{wp}):

$$ET_{veg} = PE_{veg}\left(\frac{S_{t-1} - S_{wp}}{S_{fc} - S_{wp}}\right) \quad (13)$$

$$E_{soil} = PE\left(\frac{S_{t-1} - S_{wp}}{S_{fc} - S_{wp}}\right) \quad (14)$$

- if S_{t-1} is lower than the volume of water stored in the soil at the wilting point: $ET_{veg} = 0$ and $E_{soil} = 0$.

PE is estimated using the approach by Oudin et al. (2005) that only requires temperature and latitude as inputs. It was chosen given its better performance over 25 existing *PE* formulae when used as input to four hydrological models for over 300 catchments.

During evaporation of water stored on the surface of the canopy, transpiration is assumed to be negligible; hence the potential evapotranspiration of the vegetated fraction (PE_{veg}, mm) is:

$$PE_{veg} = PE - PI \quad (15)$$

Saturation excess runoff is generated by rainfall falling on areas that are saturated, i.e. *Rf* plus S_{t-1} is higher than the porosity of the soil. Given the difficulty of determining the most restrictive layer or groundwater depth, the effective hydrological depth within which the storage of water affects the generation of surface runoff is assumed to approximate the depth of the A-horizon (Morgan et al., 1984, Morgan, 2001).

To simulate deep percolation (*Dp*) we used the method applied in the BUDGET model (Raes, 2002):

$$Dp = d_s\,\tau\;(\theta_{sat} - \theta_{fc})\,\left(\frac{e^{(\theta_i - \theta_{fc})} - 1}{e^{(\theta_{sat} - \theta_{fc})} - 1}\right) \quad (16)$$

where d_s is the depth of the soil A-horizon in mm, τ is a drainage parameter, θ_i is the soil moisture at cell *i* (expressed as mm of water depth / mm of soil depth), θ_{sat} is the soil moisture at saturation, θ_{fc} is the soil moisture at field capacity. λ is given by Eq. 17:

$$0 \leq \tau = 0.0866e^{0.8063log_{10}(K_{sat})} \leq 1 \quad (17)$$

in which K_{sat} is the saturated hydraulic conductivity (mm d^{-1}).

Soil saturation, overland flow and sediment contributing areas

The concept of the soil-topographic index (Beven, 1986) is applied to represent the effect of catchment topography on soil moisture and to delineate the soil saturated area. The local water deficit values obtained in the soil moisture sub-model, based on the soil and land cover type, are redistributed according to the topography by means of the TWI. Applying the approach of (Ambroise et al., 1996) and assuming a parabolic transmissivity profile, the TWI value corresponding to the saturation threshold (λ_t), i.e. soil water deficit ≤ 0, is defined by Eq. 18:

$$\lambda_t = \bar{\lambda} / (1 - \bar{\delta}) \quad (18)$$

where $\bar{\delta}$ is the average value of relative soil storage deficit $\delta = 1 - \theta_i/\theta_{sat}$. $\bar{\lambda}$ is the average value of the TWI, which is defined for the parabolic transmissivity profile as:

$$\lambda_i = \sqrt{a_i / (T_{0i}\, tan\beta_i)} \quad (19)$$

where a_i is the upslope drainage area for the grid cell i (m^2) and T_{0i} is the local transmissivity at saturation (m^2 d^{-1}).

Monthly overland flow is only generated in areas where $\lambda_i > \lambda_t$, i.e. soil saturation areas. In these overland flow prone areas, monthly overland flow (*Q*; mm) is assumed to be equal to monthly effective rainfall (Rf; Eq.8). By applying this approach, areas with no overland flow do not contribute to the sediment balance, whereas saturated areas defined by TWI are considered as the main source of sediments to surface water bodies (Walter et al., 2000). Simulated soil loss from these areas is routed until it reaches a deposition area or a surface water body.

It is assumed that fine-grained particles transported by overland flow to the stream network will continue to be transported by channel flow to the catchment outlet or undergo only short-term storage on the channel bed. Net channel bed sediment storage is considered negligible relative to annual sediment flux in humid catchments because temporarily stored fine sediment may be readily remobilized and exported during subsequent flow events (Walling et al., 2002, Walling et al., 2006). This assumption may be less likely to hold if the monthly sediment flux, instead of yearly, is reported. Moreover, catchment-scale applications of MMF-TWI are limited to areas without significant channel bank erosion that experience negligible losses of fine-grained sediment to overbank deposition.

Rainfall kinetic energy

In order to compute the kinetic energy (KE; J m^{-2}) of raindrops reaching and detaching the soil, Rf (Eq. 8) is split into leaf drainage (LD; mm) and direct throughfall (DT; mm). Leaf drainage reaches the soil as flow or drips from the leaves and stems of the vegetation. LD is proportional to CC:

$$LD = Rf\ CC \tag{20}$$

Direct throughfall represents the raindrops falling directly onto the soil not covered by canopy:

$$DT = Rf(1 - CC) \tag{21}$$

The equation proposed by Brandt (1990) is applied to compute the kinetic energy of leaf drainage which is a function of LD and the plant height (h_c; m):

$$KE(LD) = LD(15.8 \times {h_c}^{0.5} - 5.87) \tag{22}$$

For canopy heights lower than 0.15 m, KE(LD) is assumed to be zero. Since raindrop terminal velocity is achieved at a height of approximately 8 m

(Satterlund and Adams, 1992) and, as stated by Brandt (1990), this equation overestimates KE for values of h_c above 8 m, PH values are limited to 8 m for woodland. This replaces the values proposed by Morgan and Duzant (2008), which range between 25-30 m and are likely to greatly overestimate *KE(LD)*.
Direct throughfall (DT) kinetic energy is determined from:

$$KE(DT) = DT(8.95 + 8.44 \log_{10} I) \quad (23)$$

where KE is in J m^{-2}, DT is the monthly direct throughfall in mm and *I* is the 'intensity of erosive rain' in mm h^{-1} (Morgan and Duzant, 2008). In the present study, *I* is the average of the maximum monthly 30-minute rainfall intensity (I_{30}; mm h^{-1}) for storm events discretized using the Rainfall Intensity Summarization Tool (RIST; USDA, 2014). If this information is not available, guide *I* values provided by Morgan and Duzant (2008) for different climates can be applied. To exclude snowfall from the kinetic energy calculation, rainfall intensity is assumed to be 0 when the mean daily temperature is below -1°C. Previous work in Denmark found that varying the rain-snow temperature threshold by ±2°C around 0°C had negligible effect on rainfall energy-intensity calculations (Leek and Olsen, 2000).

In order to consider the effect of the understorey interception on KE in woodland areas, the effective rainfall (Rf; mm) is divided into understorey leaf drainage (LD_{us}), canopy tree leaf drainage (LD_{tree}) and direct throughfall (*DT*). LD_{us} is defined by:

$$LD_{us} = Rf\ CC_{us} \quad (24)$$

based on Morgan and Duzant (2008), while DT is calculated by removing the proportion of tree leaf drainage reaching the soil surface though the understorey gaps:

$$DT = (Rf - LD_{us})\ (1 - CC_{tree}) = Rf(1 - CC_{us})(1 - CC_{tree}) \quad (25)$$

Therefore, LD_{tree} is:

$$LD_{tree} = Rf - LD_{us} - DT = Rf(1 - CC_{us})\, CC_{tree} \quad (26)$$

Detachment of soil particles

MMF-TWI applies a modified approach to simulate the detachment of soil particles by incorporating the effect of ground cover. We apply the surface ground cover subfactor (*SC*) used in the C-factor of RUSLE (Renard et al., 1991):

$$SC = e^{-0.035\, M} \quad (27)$$

where *M* is the percentage of mulch/plant litter and contact vegetation/roots covering the fraction of soil not covered by stones or exposed bedrock. Guide annual values of GC provided in Table III in Morgan and Duzant (2008) can be used as *M* in the absence of measured values. In order to represent tillage practices for arable land, a tillage factor applied in the C-factor of RUSLE (Faist Emmenegger et al., 2009, Stone and Hilborn, 2011, Siegerist and Pfister, 2013, Panagos et al., 2015) is applied here to SC. The values of the tillage factor (TF) depend on the tillage practice used:

- TF = 1.00 for conventional tillage;
- TF = 0.35 for conservation/ridge tillage;
- TF = 0.25 for no till practices.

If more detailed information about the tillage practices is available, the method proposed by Stone and Hilborn (2011) to obtain TF can be applied. This method splits the TF into subfactors, the tillage method subfactor (TMF) and the support practice subfactor (SPF), being TF = TMF × SPF. TMF represents tillage method for the crop to be grown and SPF represents the effects of tillage practices that reduce the amount and rate of the water runoff, such as cross-slope or contour tillage, and thus reduce the amount of erosion. Guide values for TMF and SPF are proposed by Stone and Hilborn (2011) (see Table VI and Table VII in Appendix).

Thus, the equation based on MMF (Morgan, 2001, Morgan and Duzant, 2008) to predict soil detachment by rainfall (F; kg m^{-2}) of clay (i = c), silt (i = z) or sand (i = s) is as following:

$$F_i = K_i \frac{\%i}{100} (SC\ TF) (1 - ST) KE\ 10^{-3} \quad (28)$$

where K_i is the detachability of the soil (J m^{-2}), ST the stone or bedrock cover, $\%i$ is the percentage of clay (c), silt (z) or sand (s). The equation based on MMF (Morgan, 2001, Morgan and Duzant, 2008) to predict soil detachment by overland flow (H; kg m^{-2}) of clay (i = c), silt (i = z) or sand (i = s) is as following:

$$H_i = DR_i \frac{\%i}{100} Q^{1.5} (SC\ TF) (1 - ST) sin^{0.3}\beta\ 10^{-3} \quad (29)$$

where DR_i is the detachability of the soil by overland flow (g mm^{-1}) and Q is the monthly volume of overland flow (mm).

Immediate deposition of detached particles

A proportion of the detached particles are immediately deposited close to the point of detachment due to gravitational force (DEP) and the remainder are delivered to the overland flow for transport. Deposition is a function of the fall number (N_f; (Tollner et al., 1976), which is a function of the element length (l; m), the particle settling velocity (v_s; m s^{-1}), the flow velocity (v; m s^{-1}) and the flow depth (d; m):

$$DEP\ (i) = 0.441\ (N_f(i))^{0.29} = 0.441 \left(\frac{l\ v_s(i)}{v\ d}\right)^{0.29} \quad (30)$$

where d is 0.005 m for unchanneled flow, 0.01 m for shallow rills, and 0.25 m for deeper rills; v_s is 2 × 10^{-6} m s^{-1} for clay, 2 × 10^{-3} m s^{-1} for silt, and 2 × 10^{-2} m s^{-1} for sand (Morgan and Duzant, 2008); and v is calculated, as proposed by (Choi

et al., 2017), by means of the Manning's roughness coefficient (*n'*) from Petryk and Bosmajian (1975), which considers the drag force by vegetation in addition to the Manning's roughness coefficient of the soil (*n*):

$$v = \frac{1}{n'} d^{2/3} \sqrt{tan(\beta)} \tag{31}$$

$$n' = \left(n^2 + \frac{D\ NV\ d^{4/3}}{2g} \right)^{1/2} \tag{32}$$

where D is the diameter of plant stems in metres and NV is the number of stems per unit area. A value of n = 0.015 is recommended for bare soil (Morgan and Duzant, 2008). In woodland environments, in order to capture the effect of woodland understorey MMF-TWI adds the *D* x NV product of the understorey to the value of *D* x NV of woodland (Table X in Appendix). In non-saturated areas where no overland flow is generated, DEP is equal to 1.

Sediment production

The amount of particles (G; kg m^{-2}) of clay ($i = c$), silt ($i = z$) or sand ($i = s$) available for transport is computed as:

$$G(i) = (F(i) + H(i))(1 - DEP(i)) + SL(CE)(i) \tag{33}$$

where SL(CE) is the input of material in the overland flow from the contributing upslope grid cells in kg m^{-2}. MMF-TWI uses the flow direction algorithm D∞ (Tarboton, 1997) for routing the sediment flux from the contributing upslope grid cells.

Transport capacity

The transport capacity of the overland flow (TC; kg m^{-2}) is computed as a function of the volume of runoff, slope steepness and the effect of surface cover and tillage practices. In the same way as for rainfall and runoff detachment, the surface cover and tillage effects are represented by SC and TF respectively. The equation based on MMF (Morgan, 2001) to compute TC of clay (*i* = *c*), silt (*i* = *z*) or sand (*i* = *s*) is:

$$TC(i) = (SC\ TF)\ \frac{\%i}{100} Q^2\ sin\,\beta\ 10^{-3} \quad (34)$$

This approach is similar to the one applied by the RMMF model (Morgan, 2001) where the surface cover and tillage effects are represented by the complete C-factor of RUSLE, which also includes representation of the previous land use (PLU), canopy cover (CC), soil roughness (SR) and soil moisture (SM) effects (Renard et al., 1997). However, since CC and SM are already represented in the MMF-TWI model and the PLU and SR by TF they are not included in the TC computation.

In the MMMF model (Morgan and Duzant, 2008) the C-factor was replaced by a flow velocity ratio in the TC equation. However, this approach was discarded because it assumes that more intensive tillage practices produce less soil loss. This approach in MMMF was corrected by (Choi et al., 2016) and represents tillage practices as a factor that increases soil roughness with tillage intensity and as a consequence reduces flow velocity and hence TC. In other words, more intensive tillage practices yield lower TC and lower soil loss compared to more conservative tillage practices. As a consequence, this approach does not reflect the effect of conservative tillage and no-tillage practices in minimizing soil erosion by reducing the soil disturbance and allowing more surface residue (Busari et al., 2015). The MMMF approach does not take into account the direction of tillage or that roughness elements created by tillage, especially when parallel to the slope, can concentrate flow in non-permanent channels, thereby increasing the erosion and sediment transport capacity of the flow (Govers et al., 2000, Kirkby et al., 2002, Gómez and Nearing, 2005, Peñuela et al., 2016).

Sediment flux

In order to compute the sediment loss at each grid cell (SL; kg m^{-2}) and the sediment delivery, TC is compared to *G*. If the transport capacity is higher than the detached particles available for transport, then all G is transported from the grid cell and the soil loss is equal to *G*.

$$If\ TC(i) > G(i), SL(i) = G(i) \tag{35}$$

If TC is lower than *G*, sediments will be deposited from *G* until TC is equal to *G*.

$$If\ TC(i) < G(i), \text{calculate}\ \ G(i1) = G(i)\big(1 - DEP(i)\big) \tag{36}$$

$$If\ TC(i) \geq G(i1), SL(i) = TC(i);\ if\ TC(i) < G(i1), SL(i) = G(i1) \tag{37}$$

Eq. 30 is applied to compute DEP, but instead of applying settling velocities (v_s) for overland flow on hillslopes. Morgan and Duzant (2008) recommend the following values of v_s to compute DEP in Eq. 36: 2×10^{-5} m/s for clay, 2×10^{-2} m/s for silt and 2×10^{-1} m/s for sand. In non-saturated areas and hence where no overland flow is generated, DEP is equal to 1. This is an important condition because it avoids a possible disconnection between the overland flow and the sediment flux processes. In MMMF, since DEP depends on the flow velocity but not on *Q*, areas where *Q* and hence *H* are equal to 0 but *F* and hence *G* are higher than 0 could appear as sediment contributing areas since G(*i*1) > 0 and SL(*i*) = G(*i*1) according to Eq. 37, even though TC = 0.

Model evaluation and comparison

An extensive validation of the model is beyond the scope of this initial paper which focuses on model description. This section is rather intended to evaluate MMF-TWI performance by first comparing model results to data available from measurements in the UK and to results obtained by the most recent version of MMF, the Modified MMF (MMMF), and second by assessing the ability of MMF-TWI to capture the effects of land cover type and its spatial and temporal

variability on sediment flux. More extensive field applications and model validation are intended for subsequent publications.

Study catchment

MMF-TWI was applied in an agricultural catchment (48 km^2) draining into the Loch of Skene in northeast Scotland. The catchment ranges in elevation from 82 to 428 m (Figure 3a). The lake is shallow, has an area of 1.14 km^2 and is eutrophic, mainly due to intensive agricultural practices in the last century (Cooksley, 2007).

Land cover is predominantly agricultural, with a mixture of pasture (50%), arable land (26%), and woodland (18%) based on aerial imagery from 2007 (Figure 3b). The dominant crop is spring barley. For the purpose of comparing model simulations, we assume post-harvest winter cover crops are grown each year, with no inter-year change in land cover, and conventional tillage practices. Optimal growth conditions are assumed for the cover crop which is planted immediately after the barley harvest. Soils are sandy clay loams. Soil parameters were derived from data supplied by the James Hutton Institute. Based on the soil texture, pedotransfer functions (Hollis et al., 2015) were used to estimate soil hydraulic parameters. The SWAT model crop database was used for crop parameter values (Arnold et al., 2012).

Climate data comprises 30 years (1980-2009) of daily rainfall and mean daily temperature data from Dunecht House station (3.4 km from the lake) and Dyce station (10.5 km from the lake), respectively, and 21 years (1994-2015) of sub-hourly rainfall data from Westhill station (6 km from the lake). The mean temperature and rainfall between 1980 and 2009 were 8.2 °C and 798 mm respectively. The average intensity of erosive rain ranged between 4.1 mm h^{-1} in March to 13.3 mm h^{-1} in August.

Model results

Monthly and annual simulation results for MMF-TWI show clear correlation between the overland flow generated and the sediment export (Figure 4). The

mean annual soil loss map for the simulation period indicates that higher soil loss rates (in red) are mostly located in arable fields within saturated areas (Figure 5a). Monthly soil loss outputs from saturated contributing areas are compared for August (Figure 6a) and November (Figure 6b) 1995 and highlight the seasonal variability in both erosion rates and sediment contributing areas captured by MMF-TWI.

Comparison with published data

MMF-TWI performance was evaluated by comparing model results to data available from regional measurements of catchment sediment yields. Duck (1996) reported sediment yields and areas for 11 large catchments (216 – 2861 km^2) in eastern Scotland. On the basis of fitted regression lines and assuming an organic content of 15%, a typical value observed in the sediment exported from several catchments in Scotland (Duck and McManus, 1990), the predicted sediment yields for the Loch of Skene catchment were 0.021 t ha^{-1} y^{-1} and 0.035 t ha^{-1} y^{-1} based on data for Moray Firth and northeast Grampians, respectively. The MMF-TWI simulated sediment yield of 0.023 t ha^{-1} y^{-1} falls within the range of these predicted values. This simulated sediment yield value is also consistent with estimated rates of sediment delivery to watercourses reported by the Soil Survey of England and Wales (SSEW) based on 1700 eroded arable fields across 17 localities in England and Wales between 1982 and 1986 (Evans, 1985). The reported values range between 0.01 and 0.19 t ha^{-1} y^{-1} with a mean value of 0.05 t ha^{-1} y^{-1} (Evans, 2006).

The MMF-TWI simulated gross soil erosion rates were compared to field-scale soil erosion rates on arable land reported by the SSEW. The range of values of soil erosion in MMF-TWI varies between 0 and 5.8 t ha^{-1} y^{-1}, which is consistent with the SSEW study where the range in mean annual values was 0.6-6.8 t ha^{-1} y^{-1} (Evans et al., 2016). The SSEW mean soil erosion rates for spring and winter barley are 1.75 m^3 ha^{-1} y^{-1} and 1.85 m^3 ha^{-1} y^{-1} respectively (Boardman, 2013), or 2.3 t ha^{-1} y^{-1} and 2.4 t ha^{-1} y^{-1} respectively assuming soil bulk density of 1.3 g cm^{-3}, while the simulated value is 1.9 t ha^{-1} y^{-1} for spring barley (Table I) and 2.1 t ha^{-1} y^{-1} for winter barley with post-harvest cover crops.

For grassland and woodland areas, no regional published data are available to compare with simulated soil erosion rates. Instead, an extensive database of erosion rates measured on erosion plots in Europe compiled from the literature (Cerdan et al., 2010) was used for comparison with simulated values. According to this database, the mean soil erosion rates (± standard deviation) measured in grassland and woodland areas in Europe are 0.30 ± 1.1 and 0.14 ± 0.2 t ha^{-1} y^{-1}, respectively. These values are consistent with simulated rates of 0.61 for lowland grass and 0.21 t ha^{-1} y^{-1} for woodland (coniferous; Table I).

While no regional measurements of surface runoff are available, plot measurements obtained in European temperate regions were used for comparison with simulated runoff ratios. According to a database that comprises 227 plot-measuring sites in Europe and the Mediterranean (Maetens et al., 2012), in temperate regions the mean surface runoff ratio ranges between 1.1% for grasslands and 5.2% for bare soils. This is consistent with the simulated mean value of 3.3% for overland flow in the study catchment.

Comparison with Modified MMF model (MMMF)

MMF-TWI and MMMF produce comparable soil erosion rates for spring barley and grassland (Table I). However, MMMF simulates very high soil erosion rates in woodland areas, over 9.8 t ha^{-1} y^{-1}, compared to rates simulated by MMF-TWI and values reported in the literature (Cerdan et al., 2010). Unlike MMF-TWI, where the highest soil loss values occur on arable land (Figure 5a), in MMMF the main sediment contributing land use is woodland (Figure 5b). This produces an annual sediment flux of 1508 t y^{-1}, which is over ten times higher than MMF-TWI (112 t y^{-1}). In woodland areas MMMF simulates very high KE for leaf drainage (38870 J m^{-2} y^{-1}) as a result of very high values for CC (0.95) and PH (25 m; Table III in Morgan and Duzant (2008)) and very high rainfall detachment (11.1 kg m^{-2} y^{-1}) due to the absence of the protective effect from both GC and woodland understorey. Soil erosion in MMMF is reduced but still very high, 8.3 t ha^{-1} y^{-1}, if the woodland PH value is limited to the height corresponding to raindrop terminal velocity (8 m; Satterlund and Adams (1992)).

MMF-TWI simulates mean overland flow of 26 mm y^{-1} and shows a clear correlation between overland flow and sediment yield processes (Figure 4). In contrast, overland flow simulated by MMMF is close to zero (0.1 mm y^{-1}). This represents a clear underestimation of overland flow by MMMF, which is consistent with the previously reported poor performance of the MMF model in predicting runoff (Vigiak et al., 2005, Morgan and Duzant, 2008, Choi et al., 2016). It also demonstrates a disconnection between the processes of overland flow generation and sediment delivery, given the high sediment export simulated by MMMF. Moreover, in contrast to MMF-TWI (Figure 5a), MMMF simulates sediment transport in areas of the catchment where no runoff is generated and assumes that the whole catchment is contributing to sediment delivery (Figure 5b).

Cover type and seasonality

Field-based assessments of erosion in arable land in the UK have shown that soil erosion frequency and severity is correlated with crop type and precipitation seasonality (Watson and Evans, 2007) and that sensitivity to erosion changes with planting time (Boardman, 1993, Davidson and Harrison, 1995, Boardman, 2013). We tested several different crop scenarios to evaluate the effect of crop type on catchment sediment exports. This involved re-classifying all arable fields according to each scenario in Table II. The effect on catchment-scale overland flow is minor, whereas sediment exports increases substantially when cover crops are not planted. In the absence of a cover crop, the soil is left exposed to increased rainfall detachment, particularly during the late autumn and winter period (Figure 2b and c) and as a consequence erosion and sediment yield increase. It is notable that ‘spring barley + cover crop’ and ‘winter barley + cover crop’ produce comparable results but spring barley has a considerably higher sediment yield when no cover crop is applied. This reflects the extended period during winter when spring barley fields have negligible cover (Figure 2b) creating an extended ‘window of opportunity’ for erosion (Boardman and Favis-Mortlock, 2014). Cover crops have an important effect in reducing sediment output, equating to -49% for spring barley and -23% for

winter barley. In the case of lowland grass, i.e. when 100% of arable fields were taken out of crop production, the combined effect of high canopy cover and low canopy height, high GC and high stem density (represented by NV and *D*) result in lower sediment yield than spring and winter barley. The barley crop scenarios produced 1.5-2.9 times more sediment output than lowland grass, underscoring the important contribution of cultivated fields to catchment-scale sediment supply from agricultural land.

We also examined the effect of land cover and climate seasonality by comparing MMF-TWI simulations using monthly parameter values with simulations using yearly averaged values. Table III shows that when seasonality is not considered, overland flow is only slightly less on an annual basis compared to monthly, whereas sediment yield is reduced by 14% or 27% for the cover crop and no cover crop scenarios, respectively. As an explanatory example, we chose the period from 1983 to 1986, and represented the monthly rainfall and sediment yield with (monthly) and without (annual) seasonality for 'spring barley + cover crop' (Figure 7a) and 'spring barley' (Figure 7b). When seasonality is not taken into account, years with similar annual rainfall such as 1984 (1009 mm) and 1985 (1000 mm) produce almost identical annual sediment yields (Figure 7a and b). In contrast, when seasonality is considered, the erosive effect of exceptionally wet months, such as November 1984, produces an important increase in the annual sediment yield (+31% with or +77% without cover crop, respectively, Figure 7b).

The effect of inter-year variation in canopy cover (CC) on the simulated sediment yield was evaluated by comparing the year with the highest average CC (1995) and the lowest CC (1986), which also corresponds to the coldest year. For comparison, we applied the same rainfall (1995) to both years and computed the monthly sediment yield. For most months the sediment output is almost identical except for the exceptionally wet month (September) where a difference of 0.4 in CC produced a 10% difference (6 t) in sediment yield. This shows that differences in plant growth rate and hence in temperature between years can have an effect on catchment sediment yield.

Tillage practices

The effect of conservation tillage practices is considered by comparing the simulated sediment fluxes of the single crop rotation scenario (spring barley with no winter cover crop) with: a) TF = 1 for conventional tillage, b) TF = 0.35 for conservation/ridge tillage , and TF = 0.25 for no-tillage practice. Table IV shows that while both conservative and no till practices had negligible effect on overland flow they had a large effect in reducing sediment yield by -49% and -57%, respectively, for spring barley and -39% and -45%, respectively, for winter barley.

Cover spatial arrangement

Representing variability in the spatial arrangement of catchment land cover is important for capturing the effects of longer-term changes in land cover and the strategic placement of conservation measures, such as buffer strips. To evaluate the effect of land cover spatial arrangement in MMF-TWI, sets of synthetic land cover maps were generated by a Monte Carlo simulation based on the random classification of agricultural fields as either crop or improved grassland. For this purpose, the number of synthetic maps needs to be large enough to generate results representative of the range in possible land cover arrangements. We simulate spring barely with and without cover crop and all synthetic maps have the same proportional land cover as the 2007 land cover map.

The results (Table V) show that the standard deviation of the simulated sediment yield starts to converge when a set of 25 or more synthetic maps is used. Considering the set of 50 synthetic maps as representative, Table V shows that variation in the spatial arrangement of arable land had negligible effect on overland flow. In contrast, spatial arrangement had a notable effect on sediment yield, particularly for spring barley with no cover crop. Higher sediment yields correspond to spatial configurations in which a higher proportion of arable land is located within saturated areas delineated by the TWI. The difference between the spatial configurations with the lowest and the highest sediment yield, i.e. relative range, is 14% for ‘spring barley + cover crop’

and 26% for spring barley. This use of Monte Carlo simulation to generate synthetic maps of crop cover can provide a useful measure of uncertainty in catchment sediment yields linked to spatial arrangement when this information is unavailable.

Final remarks

We present a new soil erosion model, MMF-TWI, for applications in humid agricultural environments. This model overcomes several limitations of previous versions of the MMF model, including underestimation of overland flow and overestimation of sediment yield and rainfall detachment, especially in woodland areas, as well as the disconnection between overland and sediment delivery processes. To overcome these limitations and improve representation of spatial and temporal variability of catchment hydrological processes, MMF-TWI improves representation of the protective effect of ground cover and woodland understorey and introduces important new features including; (1) representation of catchment hydrology based on a soil moisture sub-model, (2) delineation of sediment contributing areas according to the topographic wetness index (TWI), and (3) monthly computation to capture seasonality in climate and land cover. Simulations show that MMF-TWI produces results consistent with measured data reported in the literature and improves predictive ability in humid environments compared to the most recent version of MMF.

MMF-TWI is able to represent the effects of land cover type and its spatial and temporal variability. We show that this intra-year variability has a significant influence on sediment yields, particularly through the combined effect of climate and land cover seasonality. When seasonality is not taken into account soil erosion and sediment yields are dependent on the annual volume of rainfall and mean annual land cover parameters. However, erosion and sediment yields increase significantly during periods with low vegetation cover, such as the early stages of crop growth, and particularly when this low cover period coincides with wet months. Seasonal variations in temperature that affect plant growth and hence the degree to which vegetation cover protects the soil can also have an effect on catchment sediment yields. In combination, these

findings indicate that monthly soil erosion models may perform better than widely used annual-based models.

MMF-TWI retains the low computational and parameterisation needs of the original MMF. New data requirements are modest and comprise daily temperature and rainfall data, as well as soil hydraulic and plant growth parameters. MMF-TWI combines simple yet physically based equations, readily available climate data, and guide values as input parameters. The increase in computational requirements introduced by the soil moisture and plant growth sub-models is limited because neither routing nor redistribution is applied at this stage. The monthly time step for computing the overland flow and sediment phases offers an improved representation of seasonal catchment processes and farming practices yet still keeps the computational requirements sufficiently low for studies of agricultural and climate change over longer periods spanning decades to centuries. These features support the use of MMF-TWI as a tool for agricultural catchment management in humid environments and for simulating past and future changes in soil erosion.

Acknowledgements

This project was supported by a Research Project Grant (RPG-2014-154) awarded by The Leverhulme Trust. We acknowledge the data supplied by the James Hutton Institute and the British Atmospheric Data Centre (BADC) and the Scottish Environment Protection Agency (SEPA). The comments of two anonymous reviewers considerably improved the manuscript.

References

AGNEW, L. J., LYON, S., GÉRARD-MARCHANT, P., COLLINS, V. B., LEMBO, A. J., STEENHUIS, T. S. & WALTER, M. T. 2006. Identifying hydrologically sensitive areas: Bridging the gap between science and application. *Journal of Environmental Management,* 78**,** 63-76.

AMBROISE, B., BEVEN, K. & FREER, J. 1996. Toward a Generalization of the TOPMODEL Concepts: Topographic Indices of Hydrological Similarity. *Water Resources Research,* 32**,** 2135-2145.

ARNOLD, J., KINIRY, J., SRINIVASAN, R., WILLIAMS, J., HANEY, E. & NEITSCH, S. 2012. Soil and Water Assessment Tool input/output file documentation: Version 2012. *Texas Water Resources Institute TR 436***,** 662.

BERGSTRÖM, S. & SINGH, V. 1995. The HBV model. *Computer models of watershed hydrology.***,** 443-476.

BEVEN, K. 1986. Hillslope runoff processes and flood frequency characteristics. *Hillslope processes,* 16**,** 187-202.

BEVEN, K., LAMB, R., QUINN, P., ROMANOWICZ, R., FREER, J. & SINGH, V. 1995. Topmodel. *Computer models of watershed hydrology.***,** 627-668.

BEVEN, K. J. & KIRKBY, M. J. 1979. A physically based, variable contributing area model of basin hydrology / Un modèle à base physique de zone d'appel variable de l'hydrologie du bassin versant. *Hydrological Sciences Bulletin,* 24**,** 43-69.

BOARDMAN, J. 1993. The sensitivity of downland arable land to erosion by water. *Landscape sensitivity***,** 211-228.

BOARDMAN, J. 2013. Soil Erosion in Britain: Updating the Record. *Agriculture,* 3**,** 418.

BOARDMAN, J. & FAVIS-MORTLOCK, D. T. 2014. The significance of drilling date and crop cover with reference to soil erosion by water, with implications for mitigating erosion on agricultural land in South East England. *Soil Use and Management,* 30**,** 40-47.

BOSWELL, V. The influence of temperature upon the growth and yield of garden peas. Proc. Amer. Soc. Hort. Sci, 1926. 162-168.

BRACKEN, L. J. & CROKE, J. 2007. The concept of hydrological connectivity and its contribution to understanding runoff-dominated geomorphic systems. *Hydrological Processes,* 21**,** 1749-1763.

BRADEN, H. 1985. Ein energiehaushalts-und verdunstungsmodell for wasser und stoffhaushaltsuntersuchungen landwirtschaftlich genutzer einzugsgebiete. *Mittelungen Deutsche Bodenkundliche Geselschaft,* 42**,** 294-299.

BRADEN, H. 1995. *The model AMBETI: a detailed description of a soil-plant-atmosphere model*, Selbstverlag des Deutschen Wetterdienstes.

BRANDT, C. J. 1990. Simulation of the size distribution and erosivity of raindrops and throughfall drops. *Earth Surface Processes and Landforms,* 15**,** 687-698.

BUSARI, M. A., KUKAL, S. S., KAUR, A., BHATT, R. & DULAZI, A. A. 2015. Conservation tillage impacts on soil, crop and the environment. *International Soil and Water Conservation Research,* 3**,** 119-129.

CARTER, M. R. 1994. A review of conservation tillage strategies for humid temperate regions. *Soil and Tillage Research,* 31**,** 289-301.

CERDAN, O., GOVERS, G., LE BISSONNAIS, Y., VAN OOST, K., POESEN, J., SABY, N., GOBIN, A., VACCA, A., QUINTON, J. & AUERSWALD, K. 2010. Rates and spatial variations of soil erosion in Europe: a study based on erosion plot data. *Geomorphology,* 122**,** 167-177.

COOKSLEY, S. 2007. Dee catchment management plan. *Dee Catchment Partnership, Aberdeen*.

CHOI, K., ARNHOLD, S., HUWE, B. & REINEKING, B. 2017. Daily Based Morgan–Morgan–Finney (DMMF) Model: A Spatially Distributed Conceptual Soil Erosion Model to Simulate Complex Soil Surface Configurations. *Water,* 9**,** 278.

CHOI, K., HUWE, B. & REINEKING, B. 2016. Commentary on" Modified MMF (Morgan--Morgan--Finney) model for evaluating effects of crops and vegetation cover on soil erosion" by Morgan and Duzant (2008). *arXiv preprint arXiv:1612.08899*.

DAVIDSON, D. A. & HARRISON, D. J. 1995. The nature, causes and implications of water erosion on arable land in Scotland. *Soil Use and Management,* 11**,** 63-68.

DAVISON, P. S., WITHERS, P. J. A., LORD, E. I., BETSON, M. J. & STRÖMQVIST, J. 2008. PSYCHIC – A process-based model of phosphorus and sediment mobilisation

and delivery within agricultural catchments. Part 1: Model description and parameterisation. *Journal of Hydrology,* 350**,** 290-302.

DE JONG, S., PARACCHINI, M., BERTOLO, F., FOLVING, S., MEGIER, J. & DE ROO, A. 1999. Regional assessment of soil erosion using the distributed model SEMMED and remotely sensed data. *Catena,* 37**,** 291-308.

DIETRICH, W. E., WILSON, C. J., MONTGOMERY, D. R., MCKEAN, J. & BAUER, R. 1992. Erosion thresholds and land surface morphology. *Geology,* 20**,** 675-679.

DUCK, R. & MCMANUS, J. Relationships between catchment characteristics, land use and sediment yield in the Midland Valley of Scotland. Soil erosion on agricultural land. Proceedings of a workshop sponsored by the British Geomorphological Research Group, Coventry, UK, January 1989., 1990. John Wiley & Sons Ltd, 285-299.

DUCK, R. W. Regional variations of fluvial sediment yield in eastern Scotland. Erosion and Sediment Yield: Global and Regional Perspectives: Proceedings of an International Symposium Held at Exeter, UK, from 15 to 19 July 1996, 1996. IAHS, 157.

DUNNE, T. & BLACK, R. D. 1970. Partial Area Contributions to Storm Runoff in a Small New England Watershed. *Water Resources Research,* 6**,** 1296-1311.

DUNNE, T., MOORE, T. R. & TAYLOR, C. H. 1975. RECOGNITION AND PREDICTION OF RUNOFF-PRODUCING ZONES IN HUMID REGIONS. *Hydrol Sci BULL Sci Hydrol,* 20**,** 305-327.

DURÁN ZUAZO, V. H. & RODRÍGUEZ PLEGUEZUELO, C. R. 2008. Soil-erosion and runoff prevention by plant covers. A review. *Agronomy for Sustainable Development,* 28**,** 65-86.

EAGLESON, P. S. 1982. Ecological optimality in water-limited natural soil-vegetation systems: 1. Theory and hypothesis. *Water Resources Research,* 18**,** 325-340.

EVANS, R. 1985. *Water erosion in England and Wales 1982-1984*, Soil Survey and Land Research Centre.

EVANS, R. 1997. Soil erosion in the UK initiated by grazing animals. *Applied Geography,* 17**,** 127-141.

EVANS, R. 2006. Land use, sediment delivery and sediment yield in England and Wales. *Soil erosion and sediment redistribution in river catchments.* Wallingford, UK: CABI.

EVANS, R., COLLINS, A. L., FOSTER, I. D. L., RICKSON, R. J., ANTHONY, S. G., BREWER, T., DEEKS, L., NEWELL-PRICE, J. P., TRUCKELL, I. G. & ZHANG, Y. 2016. Extent, frequency and rate of water erosion of arable land in Britain – benefits and challenges for modelling. *Soil Use and Management,* 32**,** 149-161.

FAIST EMMENEGGER, M., REINHARD, J. & ZAH, R. 2009. Sustainability Quick Check for Biofuels—intermediate background report. *With contributions from T. Ziep, R. Weichbrodt, Prof. Dr. V. Wohlgemuth, FHTW Berlin and A, Roches, R. Freiermuth Knuchel, Dr. G Gaillard, Agroscope Reckenholz-Tänikon, Düendorf, Germany*.

FIENER, P., AUERSWALD, K. & VAN OOST, K. 2011. Spatio-temporal patterns in land use and management affecting surface runoff response of agricultural catchments—A review. *Earth-Science Reviews,* 106**,** 92-104.

FOSTER, I. D. L., COLLINS, A. L., NADEN, P. S., SEAR, D. A., JONES, J. I. & ZHANG, Y. 2011. The potential for paleolimnology to determine historic sediment delivery to rivers. *Journal of Paleolimnology,* 45**,** 287-306.

FRANKENBERGER, J. R., BROOKS, E. S., WALTER, M. T., WALTER, M. F. & STEENHUIS, T. S. 1999. A GIS-based variable source area hydrology model. *Hydrological Processes,* 13**,** 805-822.

GÓMEZ, J. & NEARING, M. 2005. Runoff and sediment losses from rough and smooth soil surfaces in a laboratory experiment. *Catena,* 59**,** 253-266.

GOVERS, G., TAKKEN, I. & HELMING, K. 2000. Soil roughness and overland flow. *Agronomie,* 20**,** 131-146.

HEWLETT, J. D. & HIBBERT, A. R. 1967. Factors affecting the response of small watersheds to precipitation in humid areas. *Forest hydrology,* 1**,** 275-290.

HOLLAND, J. M. 2004. The environmental consequences of adopting conservation tillage in Europe: reviewing the evidence. *Agriculture, Ecosystems & Environment,* 103**,** 1-25.

HOLLIS, J. M., LILLY, A., HIGGINS, A., JONES, R. J. A., KEAY, C. A. & BELLAMY, P. 2015. Predicting the water retention characteristics of UK mineral soils. *European Journal of Soil Science,* 66**,** 239-252.

HOUGH, M. N. & JONES, R. J. A. 1997. The United Kingdom Meteorological Office rainfall and evaporation calculation system: MORECS version 2.0-an overview. *Hydrol. Earth Syst. Sci.,* 1**,** 227-239.

KIRKBRIDE, M. P. & REEVES, A. D. 1993. Soil erosion caused by low-intensity rainfall in Angus, Scotland. *Applied Geography,* 13**,** 299-311.

KIRKBY, M., BRACKEN, L. & REANEY, S. 2002. The influence of land use, soils and topography on the delivery of hillslope runoff to channels in SE Spain. *Earth Surface Processes and Landforms,* 27**,** 1459-1473.

KROES, J., VAN DAM, J., GROENENDIJK, P., HENDRIKS, R. & JACOBS, C. 2008. SWAP version 3.2. Theory description and user manual. *Alterra report,* 1649.

LAL, R. 2001. Soil degradation by erosion. *Land Degradation and Development,* 12**,** 519-539.

LEEK, R. & OLSEN, P. 2000. Modelling climatic erosivity as a factor for soil erosion in Denmark: changes and temporal trends. *Soil Use and Management,* 16**,** 61-65.

LEXARTZA-ARTZA, I. & WAINWRIGHT, J. 2009. Hydrological connectivity: Linking concepts with practical implications. *CATENA,* 79**,** 146-152.

LI, P., MU, X., HOLDEN, J., WU, Y., IRVINE, B., WANG, F., GAO, P., ZHAO, G. & SUN, W. 2017. Comparison of soil erosion models used to study the Chinese Loess Plateau. *Earth-Science Reviews*.

LÓPEZ-VICENTE, M., NAVAS, A., GASPAR, L. & MACHÍN, J. 2013. Advanced modelling of runoff and soil redistribution for agricultural systems: The SERT model. *Agricultural Water Management,* 125**,** 1-12.

LÓPEZ-VICENTE, M., NAVAS, A. & MACHÍN, J. 2008. Modelling soil detachment rates in rainfed agrosystems in the south-central Pyrenees. *Agricultural water management,* 95**,** 1079-1089.

MAETENS, W., VANMAERCKE, M., POESEN, J., JANKAUSKAS, B., JANKAUSKIENE, G. & IONITA, I. 2012. Effects of land use on annual runoff and soil loss in Europe and the Mediterranean: A meta-analysis of plot data. *Progress in Physical Geography,* 36**,** 599-653.

MANFREDA, S., FIORENTINO, M. & IACOBELLIS, V. 2005. DREAM: a distributed model for runoff, evapotranspiration, and antecedent soil moisture simulation. *Advances in Geosciences,* 2**,** 31-39.

MERRITT, W. S., LETCHER, R. A. & JAKEMAN, A. J. 2003. A review of erosion and sediment transport models. *Environmental Modelling & Software,* 18**,** 761-799.

MEYER, L. & WISCHMEIER, W. 1969. Mathematical simulation of the process of soil erosion by water. *Trans. ASAE,* 12**,** 754-758.

MOORE, I. D., O'LOUGHLIN, E. M. & BURCH, G. J. 1988. A contour-based topographic model for hydrological and ecological applications. *Earth Surface Processes and Landforms,* 13**,** 305-320.

MORGAN, R. P. C. 2001. A simple approach to soil loss prediction: a revised Morgan–Morgan–Finney model. *CATENA,* 44**,** 305-322.

MORGAN, R. P. C. 2005. Soil Erosion and Conservation, 3rd edition. Blackwell Publishing, Oxford, 2005. x + 304 pp. ISBN 1-4051-1781-8. *European Journal of Soil Science,* 56**,** 686-686.

MORGAN, R. P. C. & DUZANT, J. H. 2008. Modified MMF (Morgan–Morgan–Finney) model for evaluating effects of crops and vegetation cover on soil erosion. *Earth Surface Processes and Landforms,* 33**,** 90-106.

MORGAN, R. P. C., MORGAN, D. D. V. & FINNEY, H. J. 1984. A predictive model for the assessment of soil erosion risk. *Journal of Agricultural Engineering Research,* 30**,** 245-253.

MORGAN, R. P. C., QUINTON, J. N., SMITH, R. E., GOVERS, G., POESEN, J. W. A., CHISCI, G. & TORRI, D. 1998. The EUROSEM Model. *In:* BOARDMAN, J. & FAVIS-MORTLOCK, D. (eds.) *Modelling Soil Erosion by Water.* Berlin, Heidelberg: Springer Berlin Heidelberg.

NEARING, M. A., FOSTER, G. R., LANE, L. J. & FINKNER, S. C. 1989. A Process-Based Soil Erosion Model for USDA-Water Erosion Prediction Project Technology. 32.

NEITSCH, S. L., ARNOLD, J. G., KINIRY, J. R. & WILLIAMS, J. R. 2011. Soil and water assessment tool theoretical documentation version 2009. Texas Water Resources Institute.

O'LOUGHLIN, E. M. 1981. Saturation regions in catchments and their relations to soil and topographic properties. *Journal of Hydrology,* 53**,** 229-246.

O'LOUGHLIN, E. M. 1986. Prediction of Surface Saturation Zones in Natural Catchments by Topographic Analysis. *Water Resources Research,* 22**,** 794-804.

OUDIN, L., HERVIEU, F., MICHEL, C., PERRIN, C., ANDRÉASSIAN, V., ANCTIL, F. & LOUMAGNE, C. 2005. Which potential evapotranspiration input for a lumped rainfall–runoff model?: Part 2—Towards a simple and efficient potential evapotranspiration model for rainfall–runoff modelling. *Journal of Hydrology,* 303**,** 290-306.

PANAGOS, P., BORRELLI, P., MEUSBURGER, K., ALEWELL, C., LUGATO, E. & MONTANARELLA, L. 2015. Estimating the soil erosion cover-management factor at the European scale. *Land Use Policy,* 48**,** 38-50.

PEÑUELA, A., DARBOUX, F., JAVAUX, M. & BIELDERS, C. L. 2016. Evolution of overland flow connectivity in bare agricultural plots. *Earth Surface Processes and Landforms,* 41**,** 1595-1613.

PETRYK, S. & BOSMAJIAN, G. 1975. Analysis of flow through vegetation. *Journal of the Hydraulics Division,* 101.

PIETOLA, L., HORN, R. & YLI-HALLA, M. 2005. Effects of trampling by cattle on the hydraulic and mechanical properties of soil. *Soil and Tillage Research,* 82**,** 99-108.

PIMENTEL, D. 2006. Soil Erosion: A Food and Environmental Threat. *Environment, Development and Sustainability,* 8**,** 119-137.

PIMENTEL, D., HARVEY, C., RESOSUDARMO, P., SINCLAIR, K., KURZ, D., MCNAIR, M., CRIST, S., SHPRITZ, L., FITTON, L., SAFFOURI, R. & BLAIR, R. 1995. Environmental and Economic Costs of Soil Erosion and Conservation Benefits. *Science,* 267**,** 1117-1123.

PROSSER, I. P., RUTHERFURD, I. D., OLLEY, J. M., YOUNG, W. J., WALLBRINK, P. J. & MORAN, C. J. 2001. Large-scale patterns of erosion and sediment transport in river networks, with examples from Australia. *Marine and Freshwater Research,* 52**,** 81-99.

RENARD, K. G., FOSTER, G. R., WEESIES, G., MCCOOL, D. & YODER, D. 1997. *Predicting soil erosion by water: a guide to conservation planning with the Revised Universal Soil Loss Equation (RUSLE)*, US Government Printing Office Washington, DC.

RENARD, K. G., FOSTER, G. R., WEESIES, G. A. & PORTER, J. P. 1991. RUSLE: revised universal soil loss equation. *Journal of soil and Water Conservation,* 46**,** 30-33.

SATTERLUND, D. R. & ADAMS, P. W. 1992. *Wildland watershed management*, John Wiley & Sons Inc.

SHARMA, A., TIWARI, K. N. & BHADORIA, P. B. S. 2011. Effect of land use land cover change on soil erosion potential in an agricultural watershed. *Environmental Monitoring and Assessment,* 173**,** 789-801.

SIEGERIST, S. & PFISTER, S. Calculating crop-dependent spatially differentiated phosphorus emissions from agriculture. Proceedings from the LCA XIII International Conference, 2013.

SMITH, H. G., BLAKE, W. H. & TAYLOR, A. 2014. Modelling particle residence times in agricultural river basins using a sediment budget model and fallout radionuclide tracers. *Earth Surface Processes and Landforms,* 39**,** 1944-1959.

STOATE, C., BOATMAN, N. D., BORRALHO, R. J., CARVALHO, C. R., DE SNOO, G. R. & EDEN, P. 2001. Ecological impacts of arable intensification in Europe. *Journal of Environmental Management,* 63**,** 337-365.

STONE, R. P. & HILBORN, D. 2011. Universal Soil Loss Equation (USLE) Factsheet Order No. 12-051. *Ministry of Agriculture, Food and Rural Affairs, Ontario, Canada*.

TARBOTON, D. G. 1997. A new method for the determination of flow directions and upslope areas in grid digital elevation models. *Water Resources Research,* 33**,** 309-319.

THOMAS, I. A., JORDAN, P., MELLANDER, P. E., FENTON, O., SHINE, O., Ó HUALLACHÁIN, D., CREAMER, R., MCDONALD, N. T., DUNLOP, P. & MURPHY, P. N. C. 2016. Improving the identification of hydrologically sensitive areas using LiDAR DEMs for the delineation and mitigation of critical source areas of diffuse pollution. *Science of The Total Environment,* 556**,** 276-290.

TIWARI, A. K., RISSE, L. M. & NEARING, M. A. 2000. EVALUATION OF WEPP AND ITS COMPARISON WITH USLE AND RUSLE. 43.

TOLLNER, E. W., BARFIELD, B., HAAN, C. & KAO, T. 1976. Suspended sediment filtration capacity of simulated vegetation. *Transactions of the ASAE,* 19**,** 678-0682.

USDA 2014. Rainfall Intensity Summarization Tool (RIST). *United States Department of Agriculture (USDA), Agriculture Research Service, National Sedimentation Laboratory, Oxford, Mississippi, Version 3.94*.

VAN OOST, K., GOVERS, G. & DESMET, P. 2000. Evaluating the effects of changes in landscape structure on soil erosion by water and tillage. *Landscape Ecology,* 15**,** 577-589.

VIEIRA, D. C. S., PRATS, S. A., NUNES, J. P., SHAKESBY, R. A., COELHO, C. O. A. & KEIZER, J. J. 2014. Modelling runoff and erosion, and their mitigation, in burned Portuguese forest using the revised Morgan–Morgan–Finney model. *Forest Ecology and Management,* 314**,** 150-165.

VIGIAK, O., OKOBA, B. O., STERK, G. & GROENENBERG, S. 2005. Modelling catchment-scale erosion patterns in the East African Highlands. *Earth Surface Processes and Landforms,* 30**,** 183-196.

WALTER, M. T., WALTER, M. F., BROOKS, E. S., STEENHUIS, T. S., BOLL, J. & WEILER, K. 2000. Hydrologically sensitive areas: Variable source area hydrology implications for water quality risk assessment. *Journal of Soil and Water Conservation,* 55**,** 277-284.

WALLING, D., COLLINS, A., JONES, P., LEEKS, G. & OLD, G. 2006. Establishing fine-grained sediment budgets for the Pang and Lambourn LOCAR catchments, UK. *Journal of Hydrology,* 330**,** 126-141.

WALLING, D., RUSSELL, M., HODGKINSON, R. & ZHANG, Y. 2002. Establishing sediment budgets for two small lowland agricultural catchments in the UK. *Catena,* 47**,** 323-353.

WATSON, A. & EVANS, R. 2007. Water erosion of arable fields in North-East Scotland, 1985 – 2007. *Scottish Geographical Journal,* 123**,** 107-121.

ZHANG, S., FAN, W., LI, Y. & YI, Y. 2017. The influence of changes in land use and landscape patterns on soil erosion in a watershed. *Science of The Total Environment,* 574**,** 34-45.

FIGURES

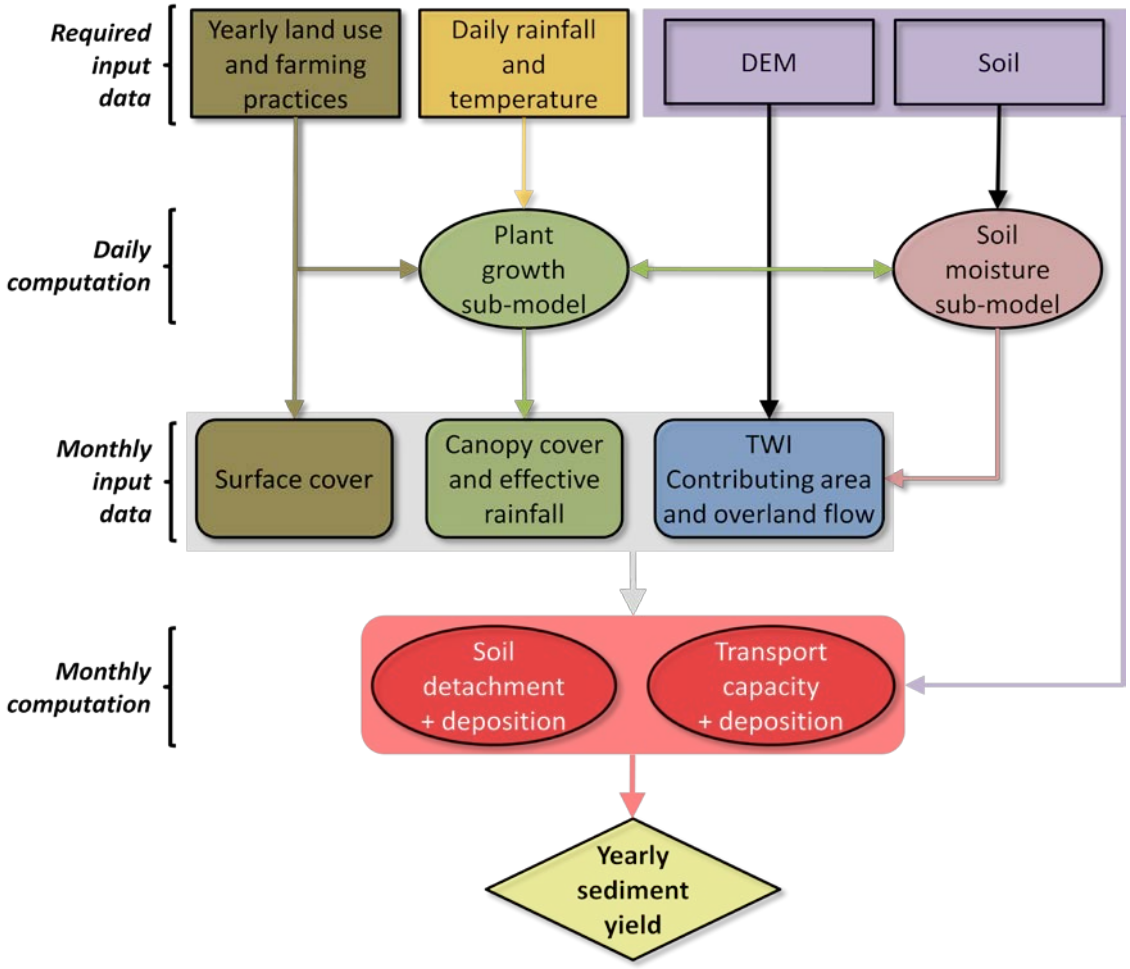

Figure 1 Schematic of MMF-TWI model framework and data requirements

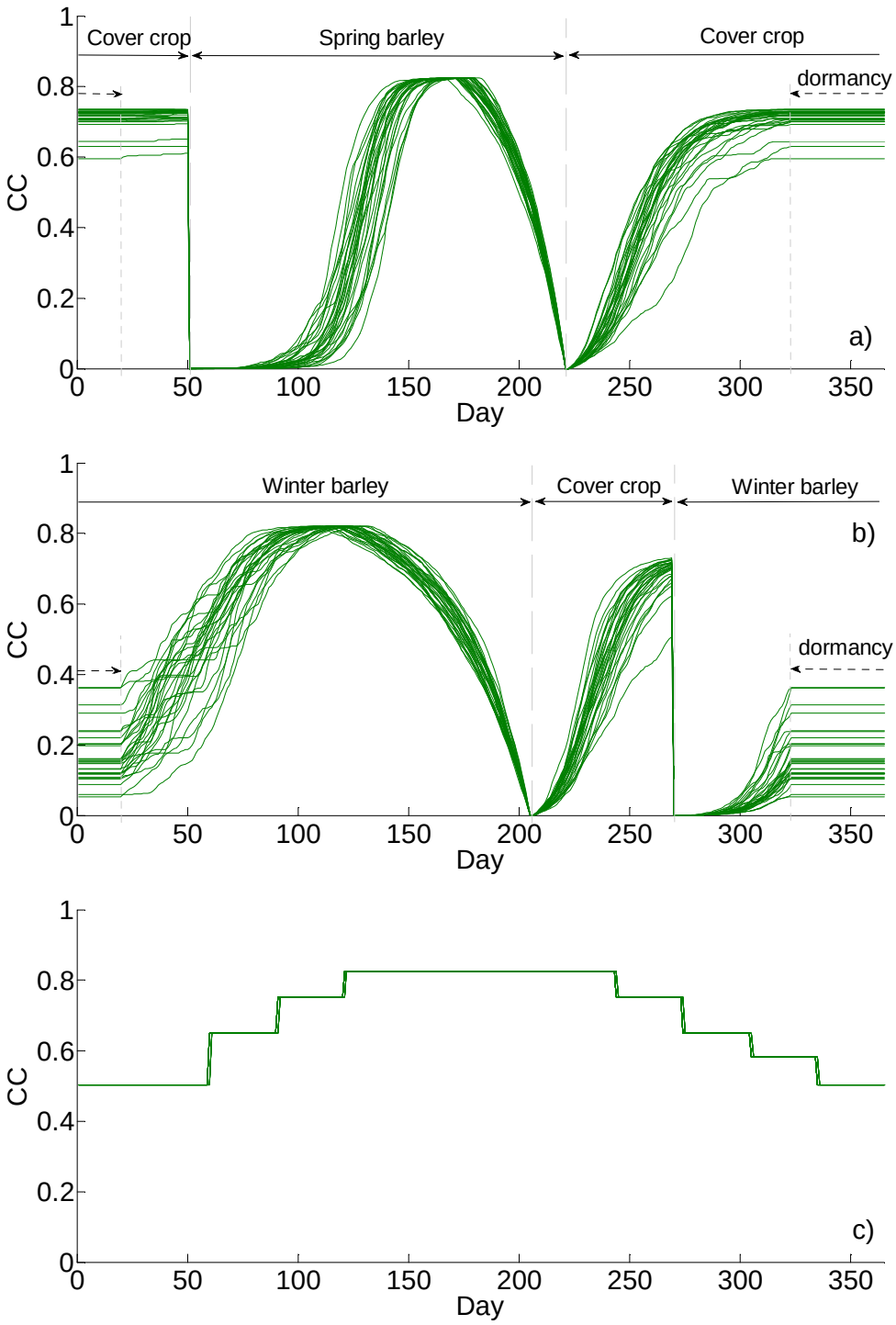

Figure 2 Canopy cover obtained from crop growth simulations for a) spring barley + cover crop, b) winter barley + cover crop and c) grassland. Each line represents a single year from 1980 to 2009.

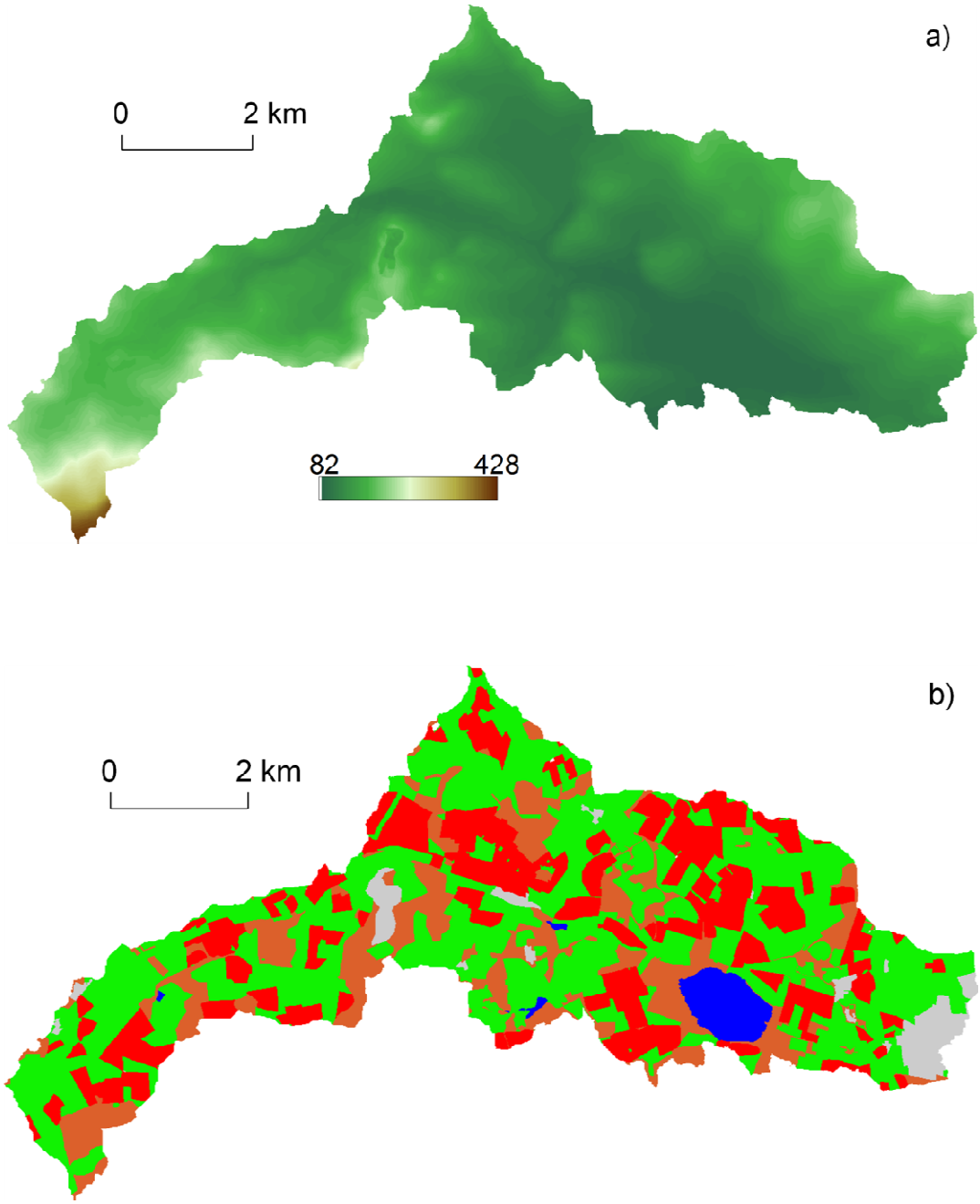

Figure 3 Loch of Skene catchment: a) Digital elevation model, in which the Loch of Skene is in black and b) 2007 land cover map, where woodland (coniferous) is in brown, improved grassland in green, arable land in red, water bodies in blue, and urban areas in cyan.

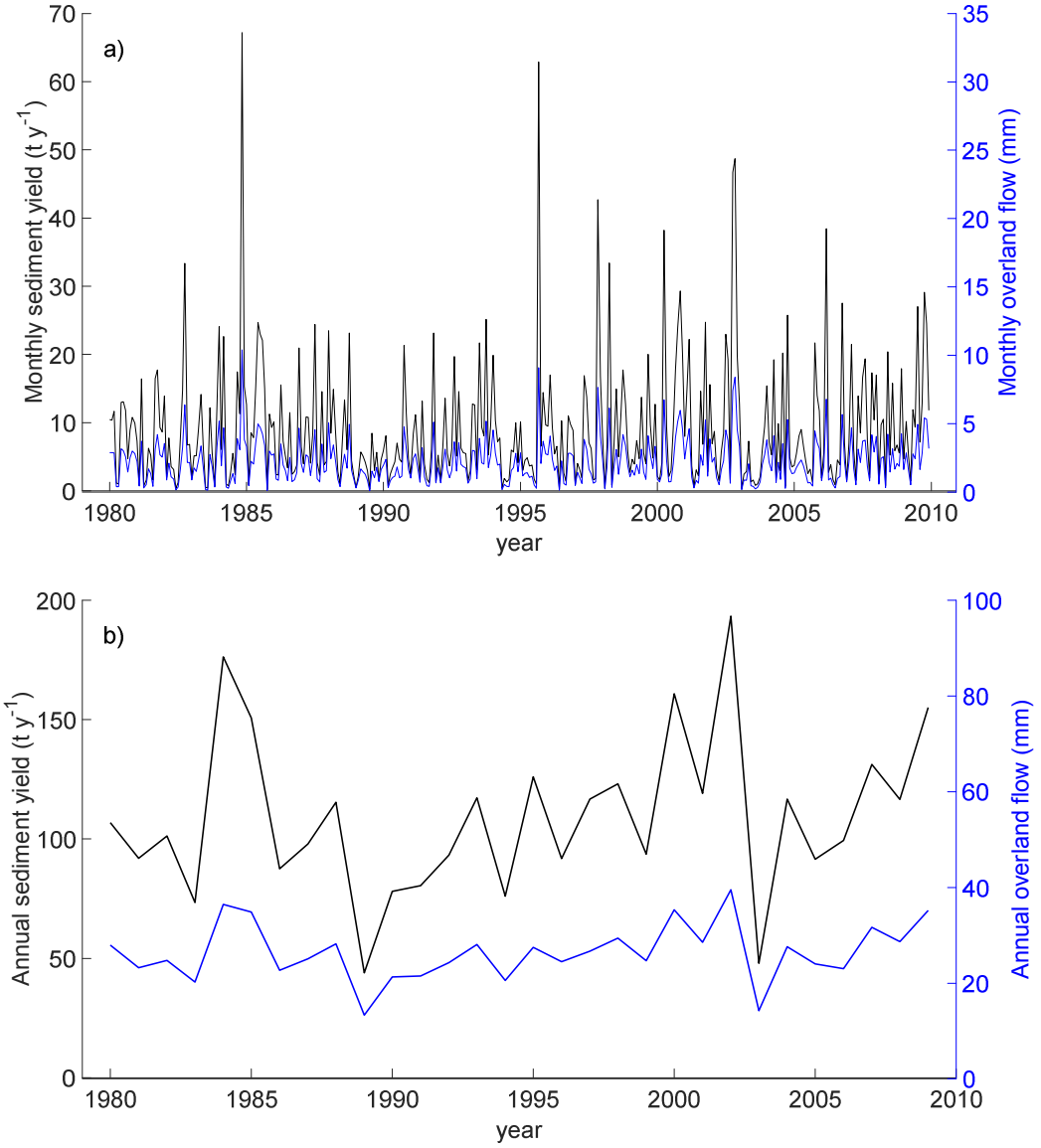

Figure 4 MMF-TWI results: a) monthly sediment yield and overland flow and b) annual sediment yield and overland flow

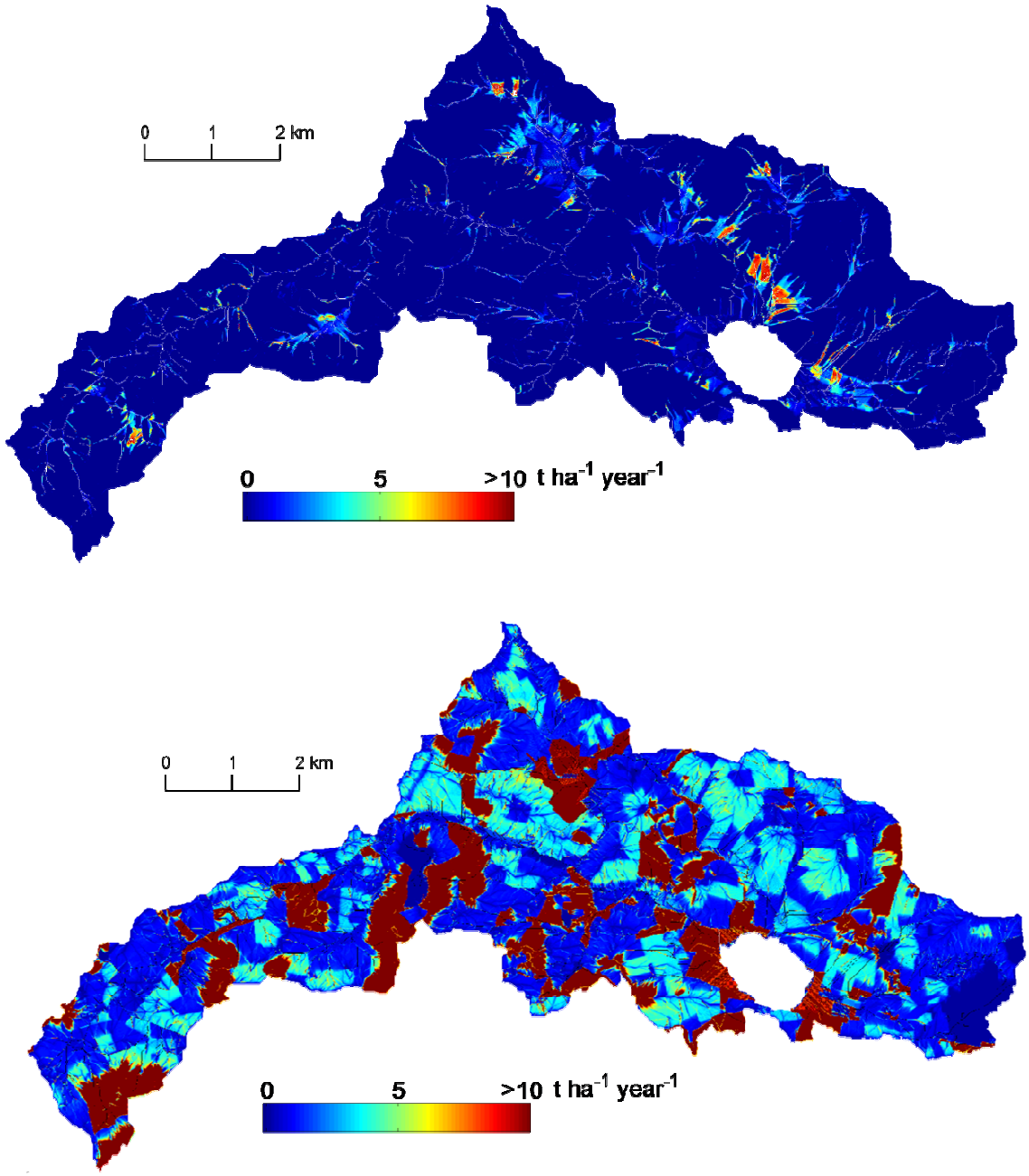

Figure 5 Mean annual soil loss map (1980-2009): a) MMF-TWI and b) MMMF.

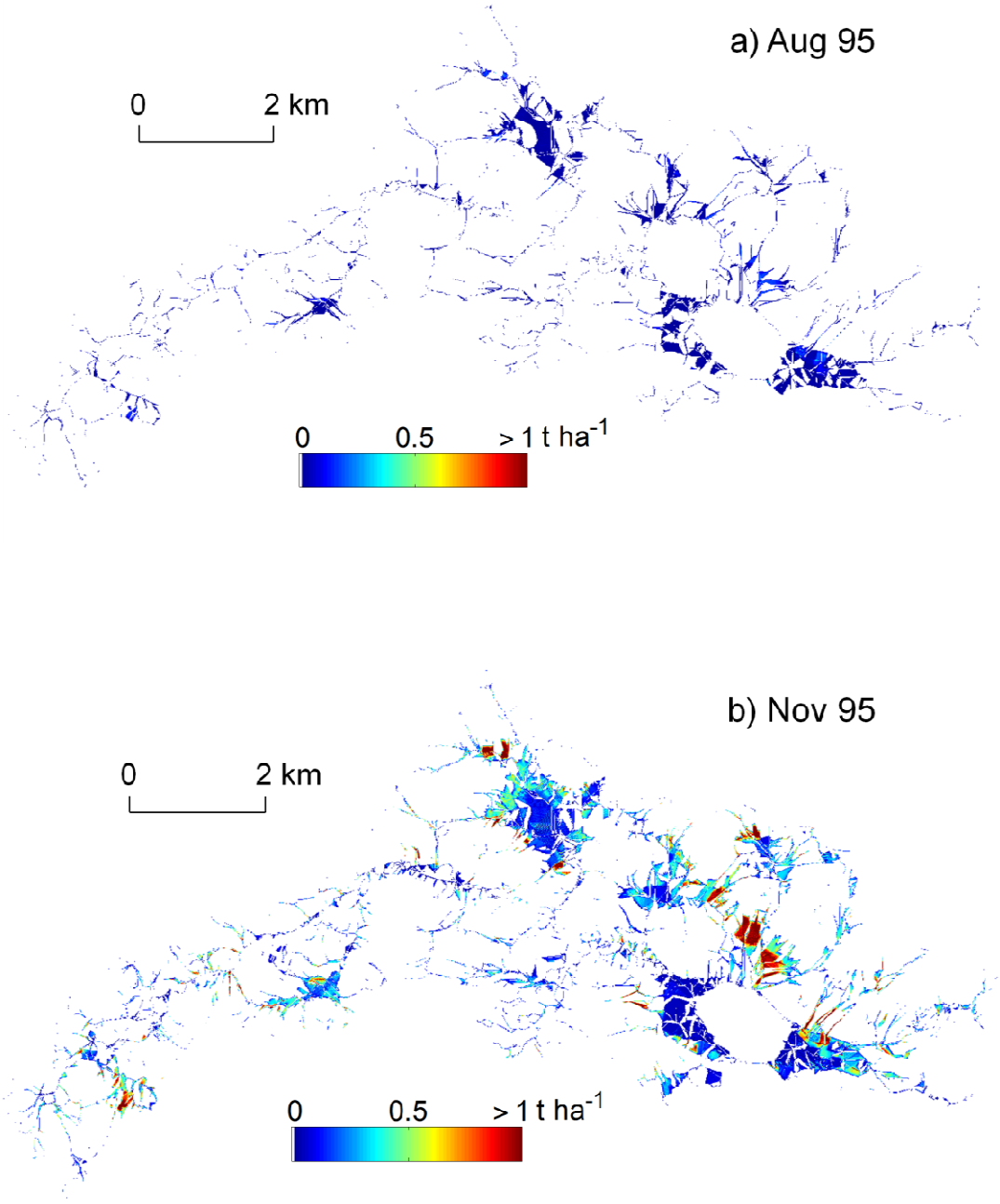

Figure 6 MMF-TWI results: monthly soil loss maps in a) August 1995 and b) November 1995. Nil values of soil loss are represented in white to highlight seasonal variation in the sediment contributing areas.

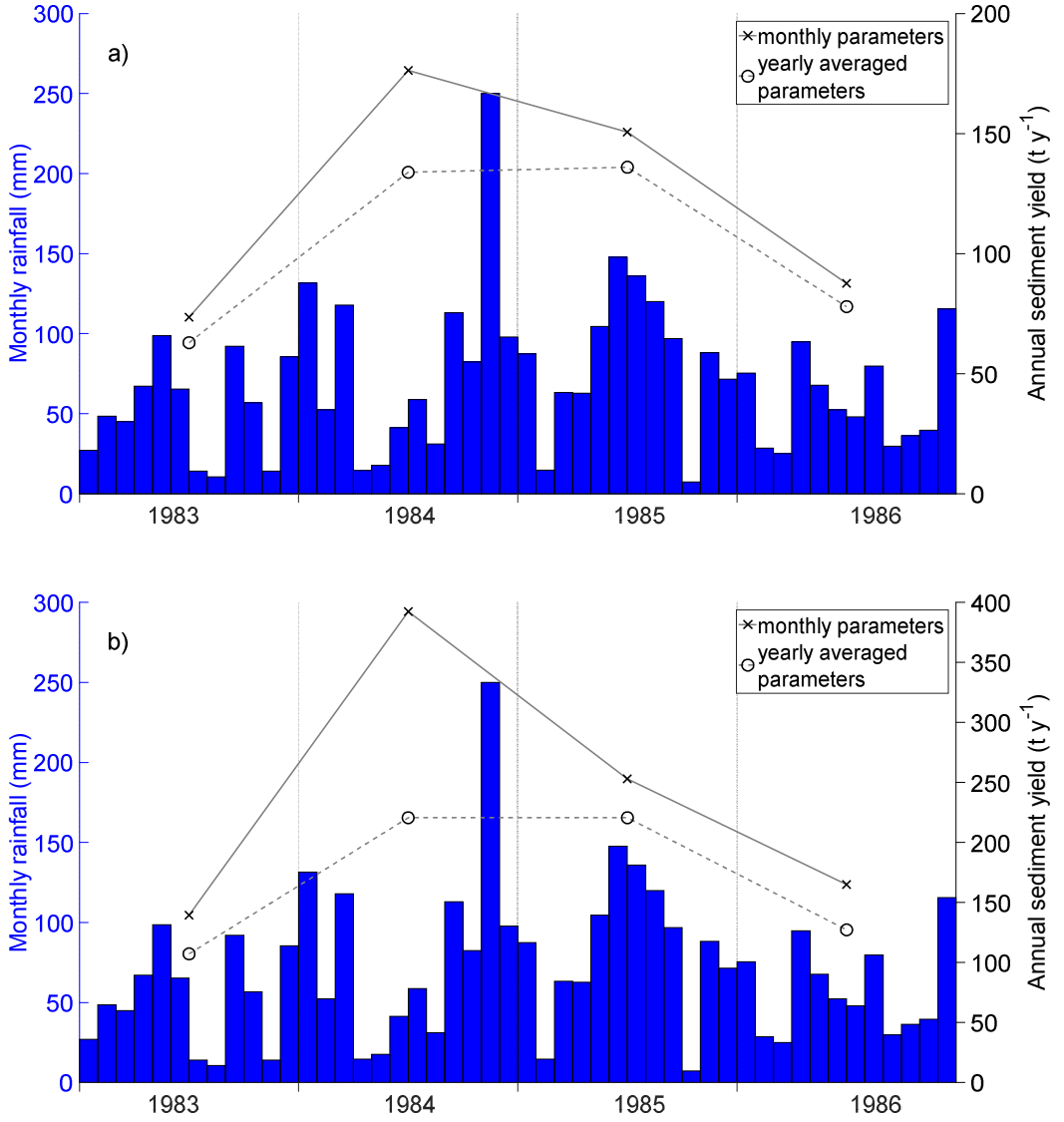

Figure 7 Land cover and climate seasonality effect: monthly rainfall and MMF-TWI simulated annual sediment yield between 1983 and 1986 when applying a) 'spring barley + cover crop' and b) spring barley only as the arable land cover.

TABLES

Table I MMF-TWI and MMMF results applying spring barley + cover crop in fields identified as arable land in the 2007 land cover map. The simulated cover crop was ryegrass.

Model output	Area	MMF-TWI	MMMF
Overland flow (mm y^{-1})	Entire catchment	26.4	0.1
Sediment yield (t y^{-1})	Entire catchment	112	1508
	Spring barley	1.91	1.59
Soil erosion rate (t ha^{-1} y^{-1})	Lowland grassland	0.61	0.42
	Woodland (coniferous)	0.21	9.8

Table II MMF-TWI results applying different crop scenarios in fields identified as arable land in the 2007 land cover map. The simulated cover crop was ryegrass.

Arable land cover	Overland flow (mm y^{-1})	Sediment yield (t y^{-1})
Spring barley + cover crop	26.4	109
Spring barley	27	216
Winter barley + cover crop	26.7	113
Winter barley	27.5	142
Lowland grass	27.1	75

Table III Land cover and climate seasonality effect: MMF-TWI simulated annual overland flow and sediment yield

Crop	Land cover and climate seasonality considered	Overland flow (mm y^{-1})	Sediment yield (t y^{-1})
Spring barley + cover crop	Yes	26.4	109
Spring barley + cover crop	No	25.2	94
Spring barley	Yes	27.0	216
Spring barley	No	25.7	156

Table IV Tillage practices effect: MMF-TWI simulated annual overland flow and sediment yield

Crop	Tillage practice	Overland flow (mm y^{-1})	Sediment yield (t y^{-1})
Spring barley	Conventional	27.0	216
	Conservation/ridge	27.0	110
	No till	27.0	94
Winter barley	Conventional	27.5	142
	Conservation/ridge	27.5	86
	No till	27.5	77

Table V MMF-TWI simulation results for n = 5, 10, 25 and 50 synthetic maps generated by randomly distributing arable fields in the Loch of Skene catchment. All generated maps have the same proportional land cover as the 2007 land cover map.

Arable land crop	n replicates	Overland flow (mm y^{-1})			Sediment yield (t y^{-1})		
		Mean	SD	Range	Mean	SD	Range
Spring barley + cover crop	5	26.5	0.1	0.2	112	5.4	14.1
	10	26.6	0	0.2	114	4.4	14.1
	25	26.6	0	0.2	115	3.9	16.3
	50	26.6	0	0.2	116	4.0	16.4
Spring barley	5	27.2	0.1	0.3	231	20.8	53.3
	10	27.2	0.1	0.3	236	16.7	53.3
	25	27.3	0.1	0.8	241	15.0	62.0
	50	27.6	0.3	1	244	15.3	63.6

Appendix A: Soil and cover parameters

Table VI Tillage method sub-factor, guide values (Stone and Hilborn, 2011).

Tillage Method	TMF
Fall plough	1.00
Spring plough	0.90
Mulch tillage	0.60
Ridge tillage	0.35
Zone tillage	0.25
No-till	0.25

Table VII Support practice sub-factor, guide values (Stone and Hilborn, 2011).

Support practice	SPF
Up & down slope	1.00
Cross slope	0.75
Contour farming	0.50
Strip cropping, cross slope	0.37
Strip cropping, contour	0.25

Table VIII Loch of Skene soil parameters (supplied by the James Hutton Institute and computed from pedotransfer functions based on Hollis et al. (2015).

SERIES name code	D (mm)	silt (%)	clay (%)	sand (%)	BD (t m^{-3})	θ_{sat}	θ_{fc} or MS	θ_{wp}	m (mm)	S_{fc} (mm)	S_{wp} (mm)	K_{sat} (mm day^{-1})	LP (m day^{-1})	T_0 (m^2 day^{-1})
Alluvial	200	16	25	59	1.408	0.44	0.34	0.18	88	68	36	1066	0.75	0.03
Blanket Peat	150	15	30	55	0.298	0.8	0.64	0.39	120	96	58.5	2804	2.07	0.12
Countesswells	150	12	22	66	0.94	0.6	0.42	0.18	90	63	27	3745	2.79	0.13
Terryvale	200	16	20	64	1.115	0.54	0.38	0.17	108	76	34	2683	1.98	0.11
Charr	200	18	15	67	0.216	0.83	0.65	0.38	166	130	76	3469	2.58	0.21

Table IX Plant growth parameters

Cover type	Planting julian date	Maturity or harvesting julian date	PHU	T_{base} (^{o}C)	$h_{c,max}$ (m)	LAI_{max}	L_1	L_2	$F_{PHU,sen}$	k
Woodland (coniferous)	n/a	n/a	n/a	n/a	8	5	n/a	n/a	n/a	0.65
Coniferous understorey	n/a	n/a	n/a	n/a	0.2	1.25	n/a	n/a	n/a	0.35
Lowland grass	n/a	n/a	n/a	n/a	0.1	5	n/a	n/a	n/a	0.35
Winter barley	270	205	1800	0	1	4	5.92	21.47	0.5	0.45
Spring barley	51	221	1570	0	1.2	4	5.92	21.47	0.6	0.45
Cover crop (annual rye grass)	n/a	n/a	1400	5	0.2	4	1.45	11.55	0.5	0.35

Table X Annual land cover parameters (Morgan and Duzant, 2008)

Cover type	EHD (m)	PI	Et/E0	CC	GC	ST	PH (m)	NV	D (m)	RFR (cm m^{-1})
Woodland (coniferous)	0.2	0.3	0.95	0.95	0.95	0.05	25	1.2	1.5	20
Coniferous understorey	n/a	n/a	n/a	n/a	1	0.05	0.2	100	0.01	20
Pasture (lowland grass)	0.12	0.3	0.86	0.9	0.6	0.05	0.1	200	0.01	20
Winter barley	0.12	0.4	0.6	0.8	0.3	0.05	1.5	250	0.05	20
Spring barley	0.12	0.3	0.58	0.8	0.3	0.05	1	200	0.04	20
Cover crop (annual rye grass)	0.12	0.3	0.86	0.9	0.6	0.05	0.1	200	0.01	20